Vol 18 No 4, April 2009
1674-1056/2009/18(04)/1473-06
Chinese Physics B
© 2009 Chin. Phys. Soc.
and IOP Publishing Ltd

Quantum-mechanical analysis of pulse reconstruction for a narrow bandwidth attosecond x-ray pulse*

Ge Yu-Cheng(葛愉成)†

School of Physics and State Key Laboratory of Nuclear Physics and Technology, Peking University, Beijing 100871, *China*

(Received 1 July 2008; revised manuscript received 17 July 2008)

The photoelectron energy spectra (PESs) excited by narrow bandwidth attosecond x-ray pulses in the presence of a few-cycle laser are quantum-mechanically calculated. Transfer equations are used to reconstruct the detailed temporal structure of an attosecond x-ray pulse directly from a measured PES. Theoretical analysis shows that the temporal uncertainties of the pulse reconstruction depend on the x-ray bandwidth. The procedure of pulse reconstruction is direct and simple without making any previous pulse assumption, data fitting analysis and time-resolved measurement of PESs. The temporal measurement range is half of a laser optical cycle.

Keywords: attosecond measurement, photoelectron energy spectrum, transfer equation, pulse reconstruction

PACC: 3365, 3280F, 3280, 3365C

1. Introduction

The dynamic process of a chemical or biochemical reaction involves energy and electron transfers which occur on femto- and attosecond time scales ($1\,\mathrm{fs}=10^{-15}\,\mathrm{s}$, $1\,\mathrm{as}=10^{-18}\,\mathrm{s}$) respectively. In order to determine how a reaction happens, increasingly shorter extreme ultraviolet (XUV) and x-ray pulses are used as pump/probe pulses. Particularly, attosecond x-rays in the water window (283.7–532.1 eV) have their own advantages in biochemical research.[1] In a cross correlation experiment where a few-cycle laser is used as an ultra-fast streak field,[2−5] an electron ionized from a gas atom via absorption of an x-ray photon carries the x-ray pulse information at the instant of ionization, and the produced photoelectron energy spectrum (PES) reflects the time properties of the pulse. The PES may be complicated due to the x-ray generation mechanism, transports, and interactions with mediums. Usually, it is difficult to explain a measured PES because of the quantum interferences between electron wave packets.

In the last decade, several methods have been developed to measure the pulse durations of attosecond XUVs.[6−14] However, we still need a direct and simple method to reconstruct the pulse from one measured PES with a high accuracy for its uses: (i) the accurate measurement of an attosecond x-ray, which is the basis of evaluating and improving the light source; (ii) the temporal structure of the pulse, which can be used as an input parameter in simulating the interaction between the pulse and atoms, and so it is important for pre-experimental analysis and detector arrangement; (iii) the detailed pulse information, which is necessary in measuring and analysing the fine structure of time-resolved x-ray absorption spectra, etc.

In our early work, we reconstructed a narrow bandwidth attosecond x-ray pulse from a semi-classically calculated PES.[15] In the present paper, photoelectron energy spectra (PESs) excited by narrow bandwidth attosecond x-rays in the presence of moderately intense few-cycle lasers ($\approx 1\times10^{14}\,\mathrm{W/cm^2}$) are investigated theoretically. The quantum-mechanically calculated PESs are compared with their classical predictions. Transfer equations which include a proportional term of a measured PES are used to determine the birth time of each photoelectron and to perform the pulse reconstruction without making any previous assumption and data fitting analysis. The temporal uncertainties of a pulse reconstruction at different times, due to the x-ray bandwidth, are calculated from an approximate formula. The method has a temporal measurement range of half of a laser optical cycle.

*Project supported by the National Natural Science Foundation of China (Grant No 10675014).
†E-mail: gyc@pku.edu.cn

2. Strong field approximation

In a cross correlation experiment, the electron motion satisfies the time-dependent Shrödinger equation in atomic units

$$\mathrm{i}\frac{\partial}{\partial t}\Psi(\boldsymbol{r},t)=\left[-\frac{1}{2}\nabla^2-\frac{1}{r}-\boldsymbol{r}E(t)\right]\Psi(\boldsymbol{r},t), \quad (1)$$

where $\boldsymbol{r}=(x,y,z)$ denotes the space coordinates; $\Psi(\boldsymbol{r},t)$ represents the electron wave function; the electric field $\boldsymbol{E}(t)=\boldsymbol{E}_L(t)+\boldsymbol{E}_X(t)$ comprises the contribution of a linearly polarized laser, $\boldsymbol{E}_L(t)=\boldsymbol{x}E_L(t)\cos(\varpi_L t-\Phi)$ (where $\boldsymbol{x}$ denotes the unit vector of the x direction, Φ is the carrier-envelope phase), and the contribution of an x-ray, $\boldsymbol{E}_X(t)=\boldsymbol{x}E_X(t)\cos(\varpi_X t)$ (x direction), with $E_L(t)$ ($E_X(t)$) being the laser (x-ray) electric field. $E_L(t)=E_0F(t)$, where $F(t)$ is the laser envelope shape peaked at time $t=0$, and E_0 is the amplitude of the laser electric field. ϖ_L and ϖ_X are laser and x-ray angular frequencies, respectively. The electric field is related to the vector potential $\boldsymbol{A}(t)$ by $\boldsymbol{E}(t)=-(1/c)\partial_t\boldsymbol{A}(t)$, where c is the speed of light.

Equation (1) can be solved analytically by applying the strong field approximation (SFA);[16,17] i.e. the Coulomb potential is neglected as compared with the laser field. As a result, the Coulomb continuum eigenfunctions can be replaced by plane waves, and equation (1) is integrated by using the expression $\Psi(\boldsymbol{r},t)=\mathrm{e}^{\mathrm{i}I_p t}\left(|0\rangle+\int\mathrm{d}^3\boldsymbol{p}b(\boldsymbol{p},t)\,|\boldsymbol{p}\rangle\right)$, where $|0\rangle$ denotes the atomic ground state with ionization potential I_p. The plane wave is given by $|\boldsymbol{p}\rangle=\exp(\mathrm{i}\boldsymbol{p}\cdot\boldsymbol{r})$, in which $\boldsymbol{p}$ is the canonical momentum of electron, and $b(\boldsymbol{p},t)$ is the momentum space wave function of free electrons. Within the SFA, the probability amplitude for transitioning from $|0\rangle$ to a final state $|\boldsymbol{p}\rangle$ reads,

$$b(\boldsymbol{p})=\mathrm{i}\int_{-\infty}^{\infty}\mathrm{d}tE(t)d_x[\boldsymbol{p}-\boldsymbol{A}(t)]\mathrm{e}^{-\mathrm{i}\tilde{S}(t)}, \quad (2)$$

where $\tilde{S}(t)$ is defined as the semi-classical action

$$\tilde{S}(t)=\int_t^{\infty}\mathrm{d}t'\left\{\frac{[\boldsymbol{p}-\boldsymbol{A}(t)]^2}{2}+I_p\right\}. \quad (3)$$

$\boldsymbol{d}(\boldsymbol{p})=\langle\boldsymbol{p}\,|\boldsymbol{x}|\,0\rangle$ is the atomic dipole matrix element for the bound-free transition, and $d_x(\boldsymbol{p})$ is the component parallel to the polarization axis: $d_x(\boldsymbol{p})=\mathrm{i}2^{19/4}I_p^{5/4}\boldsymbol{p}/\pi(2I_p+p^2)^3$ for the hydrogen bound s state ($I_p=13.6\,\mathrm{eV}$).

The PES is given by $|b(\boldsymbol{p})|^2$. We define $n(W)$, the number of photoelectrons per unit energy measured at energy W, as the PES. Practically, $n(W)=N_\mathrm{e}(W)/E_\mathrm{bin}$, where $N_\mathrm{e}(W)$ is the number of photoelectrons collected at energy W within a small size of energy bin, E_bin, e.g. 1.0, 0.5 eV or less. In theoretical calculations, we use much smaller sizes of energy bins (e.g. 0.033 eV) to illustrate how the method of pulse reconstruction works.

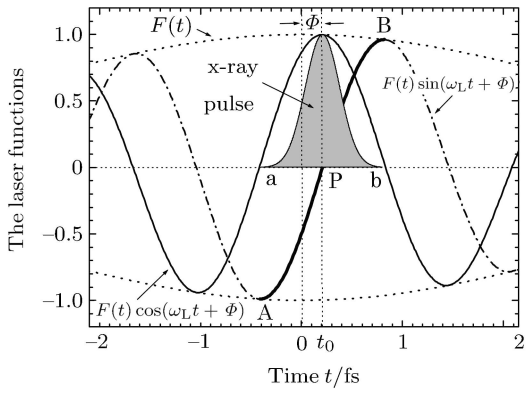


Fig.1. The laser functions, $F(t)$ (dotted), $F(t)\cos(\varpi_L t+\Phi)$ (solid) and $F(t)\sin(\varpi_L t+\Phi)$ (dashed-dotted and highlighted for half of a laser optical cycle), where the shaded Gaussian-like profile is a simple intensity distribution of the x-ray pulse.

For simplicity, a linearly polarized laser with the wavelength $\lambda_L=750\,\mathrm{nm}$ is used in schematic calculations. We define τ_L and τ_X as the pulse durations in full width at half maximum (FWHM) of the laser and x-ray, respectively. $F(t)=\exp[-4\ln 2\cdot t^2/\tau_L^2]$ is a Gaussian function with $\tau_L=7\,\mathrm{fs}$. As shown in Fig.1, a Gaussian shape x-ray pulse with $\tau_X=0.4$ fs and $\omega_X=90\,\mathrm{eV}$ is temporally centred at the time point $t_0=0.2$ fs (i.e. $\Phi=-\varpi_L t_0=-30°$). The pulse is cross-correlated to half of a laser optical cycle ($\varpi_L t+\Phi=\frac{-\pi}{2}-\frac{+\pi}{2}$, denoted by a highlighted curve segment A-P-B). Here, the instantaneous x-ray frequency ω_X is assumed to be a constant, ϖ_0, which is the central frequency of the narrow bandwidth x-ray pulse. The dotted and dashed-dotted lines in Figs.2(a) and 2(b) depict the values of PES, $n(W)$, which are quantum-mechanically calculated with different x-ray photon energies, $\hbar\varpi_0=(90,283.7)\,\mathrm{eV}$ ($\hbar$ is set to be 1 for simplicity in the following), and laser (peak) intensities, $S=(4,8,12)\times10^{13}\,\mathrm{W/cm^2}$, $\tau_X=0.150\,\mathrm{fs}$, $\Phi=0°$ and $\theta=0°$ (θ is the observation angle between the electron momentum $\boldsymbol{p}$ and the direction of linear laser polarization). We also plot the classical predictions (solid or dashed lines in Figs.2(a) and 2(b)) of each $n(W)$ for comparison. The calculations with photon energies and laser intensities in broad ranges indicate that the differences between the quantum-mechanically calculated PESs and the classical predictions are small. These tolerable differences lead us to derive the transfer equations from the classical point of view.[15]

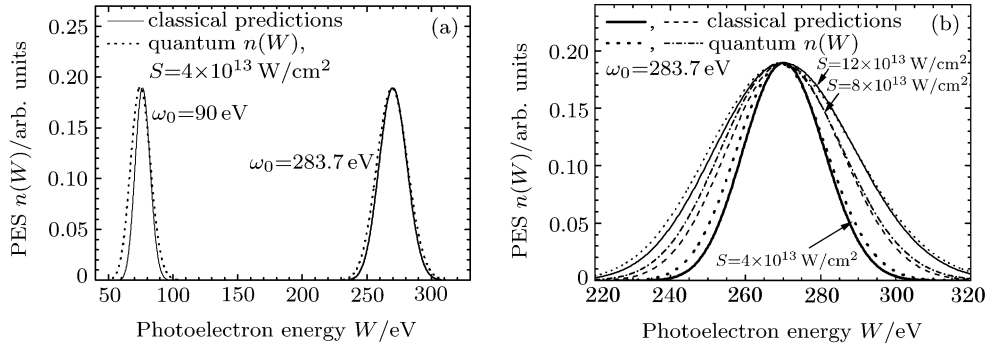


Fig.2. (a) Quantum-mechanically calculated PESs (dotted lines) excited by different energy monochromatic x-ray pulses and their classical predictions (solid lines). (b) Quantum-mechanically calculated PESs (dotted and dashed-dotted lines) and their classical predictions (solid and dashed lines), with an x-ray pulse having $\varpi_0 = 283.7\,\mathrm{eV}$ and $\tau_X = 0.150\,\mathrm{fs}$ excited and a laser having $\tau_L = 7\,\mathrm{fs}$ at different intensities modulated, and $S = (4, 8, 12) \times 10^{13}\,\mathrm{W/cm^2}$.

3. Equations for pulse reconstruction

We use the following equations to reconstruct the pulse intensity profile of a narrow bandwidth attosecond x-ray pulse.[15] To determine the photoelectron birth time t or the relevant laser phase $\varpi_L t + \Phi$ of each photoelectron of the PES, we use

$$\sin(\varpi_L t + \Phi) = \frac{\sqrt{W_{0^\circ}(t)} - \sqrt{W_{0^\circ}}}{\sqrt{2U_0}F(t)}, \qquad (4)$$

where U_0 is the ponderomotive energy of the laser field at time $t = 0\,\mathrm{fs}$, $W_0 = \varpi_0 - I_p$ is the initial energy of a photoelectron, and $W_{0^\circ}(t)$ is the final energy of the photoelectron born at t and observed at $\theta = 0^\circ$ and expressed as

$$W_{0^\circ}(t) = W_0 + 2U_0F^2(t)\sin^2(\varpi_L + \Phi) + \sqrt{8U_0W_0}F(t)\sin(\varpi_L + \Phi). \qquad (5)$$

In calculations, the spectral energy position W of PES is used instead of $W_{0^\circ}(t)$ on the right-hand side of Eq.(4).

Equation (5) is a modulation equation of the photoelectron energy and can be used to calculate the classical prediction of the PES. Solid and dashed lines in Figs.2(a) and 2(b) represent the classical predictions. They are calculated with different x-ray energies and laser intensities at $\tau_X = 0.150\,\mathrm{fs}$, $\Phi = 0^\circ$ and $\theta = 0^\circ$. These results indicate that more quantum enhancements occur at low x-ray photon energies and low laser intensities. Physically, the quantum enhancement reflects the interferences between the photoelectron wave packets generated at different times. Figures 2(a) and 2(b) show that the low energy side of a PES is more quantum-mechanically enhanced than the high energy side. As the x-ray energy and the laser intensity increase, the quantum enhancements decrease. However, both the background and the laser-induced part of the above threshold ionization (ATI) spectrum preclude the laser intensity from being increased to a very high level.[10,18] According to the simple condition,[10] i.e. $8U_0 \le \varpi_0 - I_p$, the moderate intensity $S = 1.2 \times 10^{14}\,\mathrm{W/cm^2}$ ($U_0 = 6.3\,\mathrm{eV}$) ensures that the PESs are fully separated from the ATI spectra for the x-ray frequencies concerned.

The transfer equation used to reconstruct the pulse intensity profile has a simple form as follows:

$$f(t) = \frac{\mathrm{d}W_{0^\circ}(t)}{\mathrm{d}t} \cdot \mu n(W), \qquad (6)$$

where μ is a constant and $\mathrm{d}W_{0^\circ}(t)/\mathrm{d}t$ can be theoretically calculated from Eq. (5) as follows:

$$\frac{\mathrm{d}W_{0^\circ}(t)}{\mathrm{d}t} = 2U_0\left[2F(t)\frac{\mathrm{d}F(t)}{\mathrm{d}t}\sin^2(\varpi_L t + \Phi) + 2\varpi_L F^2(t)\sin(\varpi_L t + \Phi)\cos(\varpi_L t + \Phi)\right] + \sqrt{8U_0W_0}\left[\frac{\mathrm{d}F(t)}{\mathrm{d}t}\sin(\varpi_L t + \Phi) + \varpi_L F(t)\cos(\varpi_L t + \Phi)\right]. \qquad (7)$$

Note that $\mathrm{d}F(t)/\mathrm{d}t \approx 0$ within half of a laser optical cycle around $t = 0\,\mathrm{fs}$. When $U_0 \ll 2W_0$, equation (7) can be simplified into

$$\frac{\mathrm{d}W_{0^\circ}(t)}{\mathrm{d}t} \approx \varpi_L \sqrt{8U_0W_0}F(t)\cos(\varpi_L t + \Phi). \quad (8)$$

By using Eqs. (8), equation (6) can be simplified into an approximate form as

$$f(t) \approx \varpi_L \sqrt{8U_0W_0}F(t)\cos(\varpi_L t + \Phi)\cdot \mu n(W). \quad (9)$$

Equation (6) or (9) is the transfer equation to be used to calculate the unknown temporal structure $f(t)$ from a proportional term of a measured PES, $\mu n(W)$. Usually, μ is set to be 1 for simplicity.

4. Temporal uncertainty of pulse reconstruction

Equation (5) describes the laser field modulation of photoelectron energy. Considering a small shift ΔW of the x-ray photon energy ϖ_0 or the initial photoelectron energy W_0, the final energy W_{0° of a photoelectron generated at time t will have a shift ΔW_{0°. ΔW and ΔW_{0° satisfy the following equation:

$$\begin{aligned} W_{0^\circ} + \Delta W_{0^\circ} = {} & (W_0 + \Delta W) + 2U_0F^2(t) \\ & \times \sin^2(\varpi_L t + \Phi) \\ & + \sqrt{8U_0(W_0 + \Delta W)}F(t) \\ & \times \sin(\varpi_L t + \Phi), \end{aligned} \quad (10)$$

where $W_{0^\circ} + \Delta W_{0^\circ}$ is the spectral energy position of the measured photoelectron. In fact, we use another equation to determine the photoelectron birth time $t' = t + \Delta t$,

$$\begin{aligned} W_{0^\circ} + \Delta W_{0^\circ} = {} & W_0 + 2U_0F^2(t + \Delta t) \\ & \times \sin^2[\varpi_L(t + \Delta t) + \Phi] \\ & + \sqrt{8U_0W_0}F(t + \Delta t) \\ & \times \sin[\varpi_L(t + \Delta t) + \Phi], \end{aligned} \quad (11)$$

where W_0 is used as a constant and Δt is a time shift of t. Because the values of the second and third terms on the right-hand side of Eq.(5) are much less than that of the first term, W_0, when $8U_0 \ll W_0$ (e.g. $S = 4 \times 10^{13}\,\mathrm{W/cm^2}$, $U_0 = 2.1\,\mathrm{eV}$, and $8U_0 \ll W_0 = \varpi_0 - 13.6\,\mathrm{eV} = 76.4$,270.1 eV for $\varpi_0 = 90$ and 283.7 eV, respectively), we have $\Delta W_{0^\circ} \approx \Delta W$ (see Eq.(10)). On the other hand, $\Delta W_{0^\circ} \approx \mathrm{d}W_{0^\circ}(t)/\mathrm{d}t \cdot \Delta t \approx \Delta W$ (see Eq.(11)). As a result, a bandwidth of x-ray ($\Delta\varpi_X = \Delta W$) results in a temporal uncertainty Δt of the determined photoelectron birth time. Therefore, the instantaneous temporal uncertainty of the calculated $f(t)$, due to the x-ray bandwidth ΔW, can be expressed as

$$\Delta t = \frac{\Delta W}{|\mathrm{d}W_{0^\circ}(t)/\mathrm{d}t|}, \quad (12)$$

where $\mathrm{d}W_{0^\circ}(t)/\mathrm{d}t$ is calculated from Eq.(7).

5. Calculation

To illustrate single pulse reconstructions, we use the same laser as that in Fig.1 with $\Phi = 0^\circ$. The dotted lines (overlapped by solid lines) in Figs.3(a) and 3(b) represent the profiles of initial x-ray $f_0(t)$ each with $\tau_X = 0.4\,\mathrm{fs}$, $S = 4 \times 10^{13}\,\mathrm{W/cm^2}$, $\Delta W = 5\,\mathrm{eV}$, and $\varpi_0 = 90$ and 283.7 eV respectively. The solid lines represent the intensity profiles retrieved from the quantum-mechanically calculated PESs by using transfer equations (4) and (6). The error-bar lengths represent the temporal uncertainties at different times calculated from expression (12). Note that the retrieved pulse profiles are almost the same as the initial ones (lines overlapped). These indicate that the calculations from the transfer equations give successful single pulse reconstructions.

Wide calculations with values of τ_X, ϖ_0 and S in broad ranges also show good pulse reconstructions. From Eq.(8), we have $\Delta t \propto \Delta W/\varpi_L\sqrt{8U_0W_0}F(t)\cos(\varpi_L t + \Phi)$, where $F(t) \approx 1$. The calculations show that the temporal uncertainties depend on the energy and bandwidth of the x-ray, the frequency and intensity of the laser, and the photoelectron laser phase. For example, as the x-ray bandwidth decreases, the temporal uncertainties also decrease linearly. The plots also show that the pulse reconstructions of x-rays in the water window are better than those of low energy x-rays. In addition, time jitter of the pulse and fluctuations in the experimental data may increase the background of the measured PES and the temporal uncertainties of the pulse reconstruction, but how they play a role is an interesting

topic that needs further researching. With the development of state-of-the-art laser systems, it is sure that the stabilization of the laser carrier-envelope phase, the highly accurate control of the pulse, and the decrease of the measuring time will restrict the temporal uncertainties to a low level.

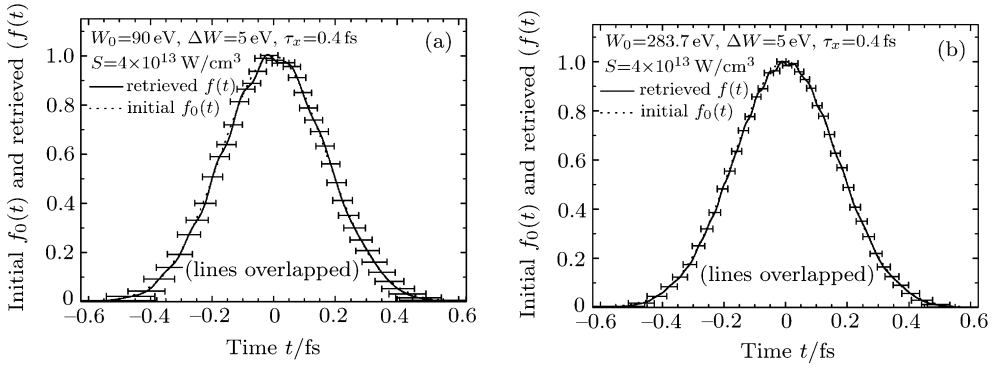


Fig.3. Single pulse reconstructions with $\tau_X = 0.4\,\mathrm{fs}$, $S = 4 \times 10^{13}\,\mathrm{W/cm^2}$, and different x-ray energies, (a) $\varpi_0 = 90$ and (b) 283.7 eV, where dotted lines represent the initial intensity profiles of the x-ray pulses, solid lines refer to retrieved intensity profiles of the x-ray pulses from the calculated PESs, and the error-bar lengths indicate the temporal uncertainties at different times calculated with $\Delta W = 5\,\mathrm{eV}$.

6. Summary

The detailed temporal structure of a narrow bandwidth attosecond x-ray (produced by any technique as long as a synchronized laser is employed) can be reconstructed directly from a measured PES by using the presented transfer equations. The measurement range is one half of a laser optical cycle. The method is capable of gaining more time information about the x-ray pulse, including possible asymmetry and side-peak structures. The following is a procedure to measure the PES and perform the pulse reconstruction: (i) measure the central energy W_0 and the energy bandwidth ΔW of the x-ray; (ii) temporally locate the x-ray pulse around $t = 0$ in a multi-shot experiment; (iii) measure the PES $n(W)$ at $\theta = 0^\circ$ with respect to the linear laser polarization; (iv) solve the photoelectron birth time t of each spectral position $W_{0\circ}$ from Eq.(4), and calculate the differential term $\mathrm{d}W_{0\circ}(t)/\mathrm{d}t$ according to Eq.(7) or (8) with the laser parameters; (v) derive the unknown temporal structure $f(t)$ of the x-ray pulse from Eq.(6) or (9); (vi) calculate the values of temporal uncertainty Δt at different times with the x-ray bandwidth ΔW from expression (12). The measurement should be repeated to achieve a high time resolution.

Acknowledgment

The author thanks Hai-Ping He for her assistance, and Prof. B. S. Zhao at the Xi'an Institute of Optics and Precision Mechanics, Chinese Academy of Sciences, D. X. Jiang, Y. L. Ye, J. X. Chen and H. T. Liu at Peking University for discussions.

References

[1] Spielmann C and Burnett N H 1997 *Science* **278** 661

[2] Drescher M, Hentschel M, Kienberger R, Tempea G, Spielmann C, Reider G A, Corkum P B and Krausz F 2001 *Science* **291** 1923

[3] Hentschel M, Kienberger R, Spielmann C, Reider G A, Milosevic N, Brabec T, Corkum P B, Heinzmann U, Drescher M and Krausz F 2001 *Nature* **414** 509

[4] Drescher M, Hentschel M, Kienberger R, Uiberacker M, Yakovlev V, Scrinzi A, Westerwalbesloh T, Kleineberg U, Heinzmann U and Krausz F 2002 *Nature* **419** 803

[5] Kienberger R, Goulielmakies E, Uiberacker M, Baltuska A, Yakovlev V, Bammer F, Scrinzi A, Westerwalbesloh T,

Kleineberg U, Heinzmann U, Drescher M and Krausz F 2004 *Nature* **427** 817

[6] Constant E, Taranukhin V D, Stolow A and Corkum P B 1997 *Phys. Rev.* A **56** 870

[7] Dinu L C, Muller H G, Kazamias S, Mullot G, Augé F, Balcou P, Paul P M, Kovačev M, Breger P and Agostini P 2003 *Phys. Rev. Lett.* **91** 063901

[8] Bandrauk A D, Chelkowski S and Shon N H 2003 *Phys. Rev.* A **68** 041802(R)

[9] Itatani J, Quéré F, Yudin G L, Ivanov M Y, Krausz F and Corkum P B 2002 *Phys. Rev. Lett.* **88** 173903

[10] Kitzler M, Milosevic N, Scrinzi A, Krausz F and Brabec T 2002 *Phys. Rev. Lett.* **88** 173904

[11] Quéré F, Itatani J, Yudin G L and Corkum P B 2003 *Phys. Rev. Lett.* **90** 073902

[12] Mairesse Y and Quéré F 2005 *Phys. Rev.* A **71** 011401(R)

[13] Sansone G, Benedetti E, Calegari F, Vozzi C, Avaldi L, Flammini R, Poletto L, Villoresi P, Altucci C, Velotta R, Stagira S, Silvestri S D and Nisoli M 2006 *Science* **314** 443

[14] Quéré F, Mairesse Y and Itatani J 2005 *J. Mod. Opt.* **52** 339

Yakovlev V S, Bammer F and Scrinzi A 2005 *J. Mod. Opt.* **52** 395

[15] Ge Y C 2006 *Chin. Phys.* **15** 2909

[16] Lewenstein M, Balcou P, Ivanov M Y, L'Huillier A and Corkum P B 1994 *Phys. Rev.* A **49** 2117

[17] Brabec T and Krausz F 2000 *Rev. Mod. Phys.* **72** 545

[18] Milosevic D B and Ehlotzky F 1998 *Phys. Rev.* A **58** 3124